

Extensive analysis of IGS REPRO1 coordinate time series

Original

Extensive analysis of IGS REPRO1 coordinate time series / Roggero, Marco. - STAMPA. - 142:(2016), pp. 81-89.
(Intervento presentato al convegno VIII Hotine-Marussi Symposium on Mathematical Geodesy tenutosi a Roma nel 17-21 June, 2013) [10.1007/1345_2015_58].

Availability:

This version is available at: 11583/2591619 since: 2021-03-18T16:32:41Z

Publisher:

Springer International Publishing AG

Published

DOI:10.1007/1345_2015_58

Terms of use:

This article is made available under terms and conditions as specified in the corresponding bibliographic description in the repository

Publisher copyright

(Article begins on next page)

Extensive analysis of IGS REPRO1 coordinate time series

M. Roggero

Abstract. The work describes the analysis conducted on the IGS REPRO1 coordinate time series, in order to detect GNSS permanent stations periodic behavior. Frequency analysis requires cyclostationary time series, while observed coordinates time series are not cyclostationary because of discontinuities of different kind and origin and of long term linear or non linear trend. For this reason time series offsets and trends must be estimated and eliminated, prior to conduct the harmonic analysis.

Discontinuities are usually documented by IGS, but undocumented discontinuities also exists and need to be detected. The long term component of the signal is generally modeled as a linear trend, but the linear model is often inadequate to obtain cyclostationary residuals. An alternative model based on a discrete time Markov process will be adopted.

The study has been conducted on the up component of the REPRO1 raw coordinates time series. No correction for the atmospheric pressure loading has been applied. Harmonic analysis has been performed using the non linear least square algorithm implemented by F. Mignard in the Frequency Analysis Mapping On Unusual Sampling software (Mignard, 2003).

We obtained a complete statistic on the vertical component period, amplitude and phase. Signals at from 1 to 7 cycle per solar and draconitic year can be observed in most stations as expected, but also other signals have been detected that can be attributed to tidal model errors. Some interpretation will be given referring to recent literature.

Keywords. Time series, REPRO1, periodic signals.

1 Introduction and motivation

Recently IGS released a first full reanalysis of all GPS data collected since 1994, the REPRO1 solution, based on the weekly SINEX solutions, from GPS week 729 (01/01/1994) to GPS week 1631 (04/16/2011). We performed a retrospective analysis of the REPRO1 coordinate time series, focusing at first on the detection, estimation, and elimination of time series offsets, than on the long term model estimation and finally on the harmonic analysis of model residuals.

Published harmonic analysis of GPS coordinates time series have shown significant variation in the respective spectrum. The most recent studies include (Ray et al., 2008), (Collilieux et al. 2007, 2010), (Fritsche et al., 2009), and (Mtamakaya et al., 2012). A comprehensive analysis of the whole REPRO1 data set¹, providing a significant and self consistent sample, can help to understand the impact of detected signals at a global scale. Moreover regional dependent spectral signatures can be observed, even if the analysis suffers of a lack of data in the southern hemisphere and in the polar areas. Coordinate and formal error time series of 526 IGS stations have been extracted from REPRO1 SINEX (ΔE , ΔN , Δh and $\sigma_N, \sigma_E, \sigma_h$) and in the present work we examined the up component (Δh , σ_h). Time series discontinuities are documented by IGS in the SOLN.SNX file, that reports 1206 documented discontinuities in position and velocity, over 338 stations (a mean of 3 or 4 discontinuities per station). The cause of about 25% of the discontinuities is unknown, while it is not possible to exclude the presence of other undocumented discontinuities. The reprocessing of IGS had been carried out by using fully consistent models in order

¹ <ftp://cddis.gsfc.nasa.gov/pub/gps/products/repro1>

to avoid model dependant discontinuities and coordinates variance anisotropy that occur in operational time series. However, the discontinuities due to hardware or monument change or to geophysical effects remain also in the reprocessed time series as noted in (Steigenberger, 2009). An example of discontinuity estimation is given in the BAKO station UP time series of Fig. 1, that presents 8 different position discontinuities reported by IGS.

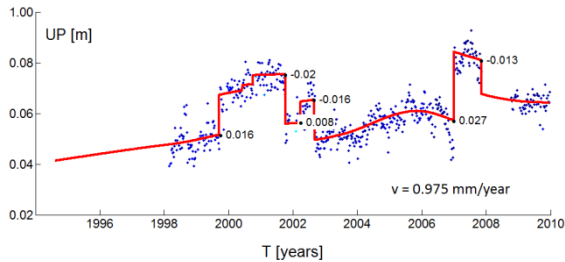


Fig. 1 – BAKO UP time series with the estimated jumps.

The changes in velocity, usually caused by earthquakes or by other geophysical effects, can be described by multi linear models, as shown in (Perfetti, 2006) and (Ostini, 2012). In these works the coordinate time series are represented as the sum of a long term linear or multi linear trend and a step function, taking in account for position offsets, and cyclical components. Harmonic analysis requires to be applied on cyclostationary residuals, having statistical properties that vary cyclically with time, however linear and also multi linear models seem to be often inadequate to describe the long term behavior of a station in order to obtain cyclostationarity, as it will be shown in par. 2.3.

To overcome the inadequacy of multi linear models applied to coordinate time series, the presented approach is based on a discrete time Markov process modeling and focuses on three steps:

1. Detect, estimate and remove the level shifts, performing iteratively the so called detection, identification and adaptation procedure (DIA) as explained in (Roggero, 2012).
2. Model the long term signal constraining the system dynamic, in order to obtain cyclostationary residuals.
3. Residuals harmonic analysis by the non linear least square algorithm implemented in the FAMOUS software (Mignard, 2003).

The step 1 of the proposed algorithm has been tested on synthetic data in the framework of the DOGEx project (Gazeaux et al. 2013). The signals estimated by FAMOUS will be analyzed in frequen-

cy, amplitude and phase, stacking the power spectra in order to detect the most significant effects. Some preliminary consideration will be given in par. 4. The software FAMOUS has been used also in (Collilieux et al. 2010) to analyze the ITRF2008, that is based on entirely reprocessed GPS solutions from 1997 to 2008.

2 Time series modeling

2.1 Discrete time linear model

GNSS time series can be modeled as discrete-time Markov process. Consider a discrete-time linear system described by a finite state vector x , evolving with known dynamics T through the epochs t ($\in t [1, n]$), with system noise v (with variance-covariance matrix R_{vv}):

$$x_{t+1} = T_{t+1}x_t + v_{t+1} \quad [1]$$

$$y_{t+1} = H_{t+1}x_{t+1} + \varepsilon_{t+1}$$

The observations y are known with observation noise ε (with variance-covariance matrix $R_{\varepsilon\varepsilon}$). It has been shown by (Albertella et al., 2006) that the system has the optimal solution

$$\hat{x} = (D^T W_\omega D + M^T W_\varepsilon M)^{-1} M^T W_\varepsilon y \quad [2]$$

where \hat{x} is the estimated state vector, D and M are block diagonal matrices representing respectively T and H over the considered time interval, while W_ω and W_ε are weight matrices. The 3D state vector \hat{x} is estimated constraining the system dynamic, by setting the system noise v at a given value. The process is detailed in (Roggero, 2008, 2012).

For a system with slow dynamic as GNSS coordinate time series, the motion can be described by a constant velocity model in T , with acceleration $\ddot{p} = 0$

$$\begin{aligned} p_{t+1} &= p_t + \dot{p}_t \cdot \delta t \\ \dot{p}_{t+1} &= \dot{p}_t \end{aligned} \quad T = \begin{bmatrix} 1 & \delta t \\ & 1 \end{bmatrix} \quad [3]$$

where the position p and the velocity \dot{p} are the two elements of the state vector $x = [p \ \dot{p}]$, with system noise $v = [v_p \ v_{\dot{p}}]$. The approach is equivalent to Kalman filtering and smoothing, but allows to manage the estimation of constant biases more efficiently, as will be shown in par. 2.2.

In state estimation the outliers are not rejected but properly weighted according to the system and observation noise.

2.2 Discontinuity model

Discontinuities has been detected, estimated and removed applying the detection, identification and adaptation procedure (DIA) presented in (Teunissen, 1998), as applied in (Perfetti, 2006) and in (Roggero, 2012). Taking in account for discontinuities requires to modify the model [1]. The bias vector b represents the time series offsets and modifies the system as follows:

$$\begin{aligned} x_{t+1} &= T_{t+1}x_t + B_{t+1}b_t + v_{t+1} \\ y_{t+1} &= H_{t+1}x_{t+1} + C_{t+1}b_t + \varepsilon_{t+1} \\ b_{t+1} &= b_t \end{aligned} \quad [4]$$

The bias vector b is constant with steps, and it is linked to the system dynamic and to the observations by the matrices B and C . The matrix C , whose elements are 0 or 1, represents the occurrence of the biases in the time series. The number of rows is equal to the number of observation epochs, while the number of columns is equal to the unknown number of jumps to be estimated. The matrix B it is assumed equal to zero if the bias affects only the observed position and not the real position. However it can be different by zero in the case of seismic displacements. These matrices can be known a priori in the case of documented discontinuities, or determined by means of some detection criteria for undocumented discontinuities. The estimation of the extended state vector $z = [x \ b]$ requires the inversion of a large sparse normal matrix. This matrix has a bordered block or band-diagonal structure (quasi-triangular Schur form), so it can thus be blockwisely inverted by using Schur decomposition as in (Roggero, 2008).

The offsets detection is based on a hypothesis test which assumes as null hypothesis H_0 that the time series do not have any offset. This hypothesis is tested against a certain number of alternative hypotheses H_A , with a jump in a given epoch. An alternative hypothesis can be formulated for each observation epoch or for candidate epochs only. The adequacy of the model can be verified using the ratio test, which is known to have the χ^2 distribution. After detecting the offsets, they can be estimated and removed.

Because offsets do not necessarily affect horizontal and vertical components similarly, the vertical component is studied separately using the same approach. This approach also makes it possible to consider documented and undocumented offsets, to predict the station coordinates in data gaps, and to correctly represent pre-seismic and post-seismic deformations or other non-linear behaviors.

The frequency analysis shows that not only the co-

ordinate time series present discontinuities in position and velocity, but also in their characteristic frequency signature. This last kind of discontinuity can be site dependant and in this case seems to be related to hardware change or to other site effects to be investigated. Model dependant frequency discontinuities can also exist, but have been avoided in REPRO1 solution by adopting models and methods fully consistent during the time.

2.3 Long term signals

In the long term signals we include the linear trend, the non linear and non periodic signals, and also the periodic signals with period larger than the time series length, that therefore are not estimable by harmonic analysis. From this point of view linear trend is only one component of the long term signal, often the larger one, but to obtain cyclostationary model residuals we can't neglect the non linear long term signals.

As we have seen in par. 2.1, the time series are modeled as a Markov process, and the system dynamic is described by a constant velocity model. A way to estimate the long term signal is by decreasing the variance σ_v of the system noise v ; in other words, the system noise is related to the maximum frequency of the estimated signal.

Because of the system noise depends on the system dynamic, the model can follow different dynamics by setting different values for the system noise variance σ_v , that has been done empirically. Fig. 2 shows the UP component time series of the ALGO station. Two different model have been estimated: model 1, with $\sigma_p = 10^{-6}$ m and $\sigma_{\dot{p}} = 10^{-5}$ m, that follows the short term signal, and model 2 with $\sigma_p = 10^{-6}$ m and $\sigma_{\dot{p}} = 10^{-6}$ m, that follows the long term signal.

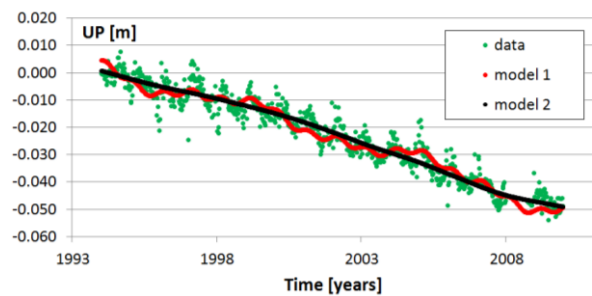


Fig. 2 – Two different variance model used to estimate the long term behavior of the ALGO station in the UP component:

- **Model 1:** short wavelength, $\sigma_p = 10^{-6}$ m and $\sigma_{\dot{p}} = 10^{-5}$ m
- **Model 2:** long wavelength, $\sigma_p = 10^{-6}$ m and $\sigma_{\dot{p}} = 10^{-6}$ m

The choice of the system variance noise is critical and depends on the sampling frequency and on the system noise. It has been fixed empirically on a sub-

set of 10 stations, randomly chosen. However the algorithm is insensitive to quite large variations of this parameter.

3 Harmonic analysis

Harmonic analysis leads to the representation of the signal as a superposition of basic waves. A variety of different approaches are presently available such as Fast Fourier transformation (FFT), Frequency Analysis Mapping On Unusual Sampling (FAMOUS) and least squares spectral analysis (LSSA). LSSA software was developed in the Department of Geodesy and Geomatics Engineering at the University of New Brunswick and it is based on the developments by (Vaníček, 1969, 1971), (Wells et al., 1985) and (Pagiatakis, 1999, 2000). However, all of them use a set of base functions made up of sine and cosine functions in the decomposition process, to generate a frequency spectrum. FAMOUS and LSSA have been developed as an alternative to bypass some of the limitations present in the classical Fourier methods. These limitations include the need for long time series, constant sampling rate, equally weighted data values, no presence of gaps or datum shifts all of which render the time series strongly non stationary.

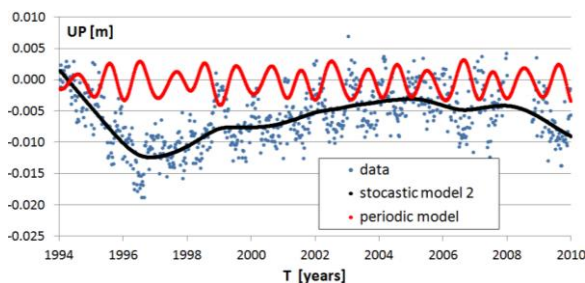


Fig. 3 - KOSG station 16 years time series, UP component. The process is clearly non cyclostationary, it presents a long term non linear behavior and a large data gap in the year 2008. The model 2 (—) with $\sigma_p = 10^{-6}$ m and $\sigma_p = 10^{-6}$ m, follows the long term behavior of the data. The periodic model (—) has been estimated by FAMOUS on the stochastic model residuals, and it is the sum of a linear component and of five different periodic signals with periods of 775.6, 527.8, 365.8, 271.0 and 41.6 days.

FAMOUS (Frequency Analysis Mapping On Unusual Sampling) makes the decomposition of a time series as

$$\psi(t) = c_0 + \sum_{i=1}^k c_i \cos(2\pi\nu_i^0 t) + s_i \sin(2\pi\nu_i^0 t) \quad [5]$$

where c_i and s_i are constant or polynomial of time:

$$c_i = a_i^0 + a_i^1 t + a_i^2 t^2 + \dots + a_i^p t^p \quad [6]$$

$$s_i = b_i^0 + b_i^1 t + b_i^2 t^2 + \dots + b_i^p t^p$$

The model

$$\min |S(t) - \psi(t)|^2 \quad [7]$$

is a non linear least square very sensitive to the starting values, solved in two steps (SVD and Levenberg-Marquardt minimization).

The solution is also given in term of $A \cos(\omega t + \varphi)$ and the signal can be reconstructed as

$$\psi(t) = c_0 + \sum_{i=1}^k A_i \cos(2\pi\nu_i^0 t + \phi_i) \quad [8]$$

FAMOUS allows the analysis of equally weighted data, with known or unknown a priori variance factors, assuming them to be uncorrelated; the algorithm can handle unevenly spaced time series without a pre-processing requirement. Tests of statistically significant spectral peaks are implemented, with respect to S/N ratio. FORTRAN source code is available by F. Mignard.

4 Analysis of IGS REPRO1 time series

Coordinate and formal error weekly time series of the full data set of 526 IGS permanent stations have been analyzed. The presented three steps procedure has been implemented in fortran90 integrating the FAMOUS source code and it is completely automatic. For this reason a complete reanalysis of REPRO1 data set takes only few minutes. The S/N threshold value for acceptance of the detected signals has been set equal to 3, as in (Collilieux et al. 2007; Mignard 2003). For each time series we obtain:

- the estimated offsets,
- the long term signal model,
- the cyclostationary residuals,
- the frequency, amplitude and phase of the detected harmonics, with their RMS.

We must note that the analysis has been conducted on the REPRO1 raw coordinates, without taking in account for atmospheric loading correction. It was been observed in (Mtamakaya, 2012) that a slight improvement to coordinates repeatability may result if Atmospheric Pressure Loading were included in the processing, however this does not cause any significant reduction in spectral peaks that are still present in the REPRO1 solutions. See also (Tregoning and Watson, 2009) for a quantitative analysis of atmos-

pheric loading. The global analysis starts from the number of detected signals over the total number of stations in [%], reported in Fig. 4. We can observe three classes of signals, related to seasonal, orbital

(draconitic) and tidal effects. The minimum sampling frequency (Nyquist frequency) for weekly time series is 14 days, at which a strong signal has been also detected, that will be attributed to tidal model errors.

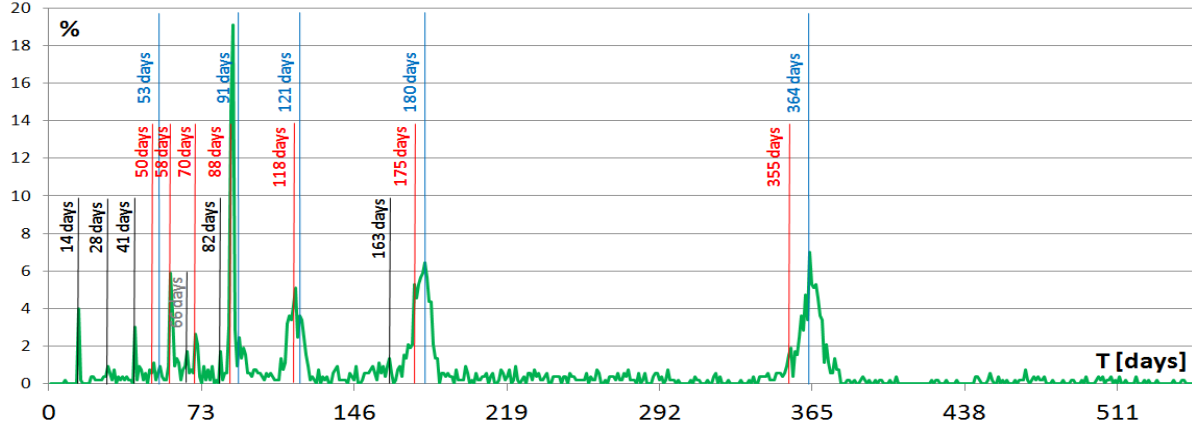


Fig. 4 – Detected signals over the number of stations in [%]. The signals evidenced in blue are the solar year harmonics (seasonal term), in red the draconitic harmonics, while in black are the tidal harmonics.

The 89% of the stations present an annual signal and signals have been detected at the 2nd, 3rd, 4th and 7th harmonics of the solar year (seasonal signals), with respective periods of 182.6, 121.8, 91.3 and 52.2 days. The annual signal amplitude, represented in Fig. 5, has a mean value of 3.1 mm and it is strongly spatially correlated. The maximum value of 1.0 cm is at the station WSLR (Whistler, Canada).

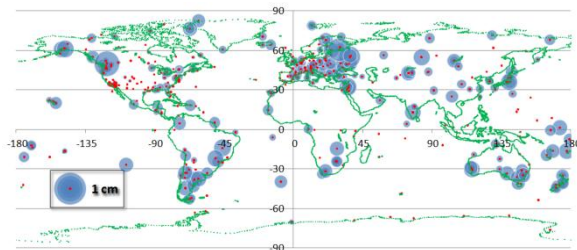


Fig. 5 - Amplitude of the annual term.

The observed signatures appear to be consistent also around the 1st, 2nd, 3rd, 4th, 6th and 7th draconitic² harmonics with respective periods of 351.2, 175.6, 117.1, 87.8, 70.2, 58.5 and 50.2 days. No signal has been detected at the higher frequencies of the

draconitic harmonics, even if some signal can be aliased by the tidal harmonics. Note in the Fig. 4 that the 1st, 2nd and 3rd draconitic harmonics overlap the 1st, 2nd and 3rd seasonal harmonics. For this reason, in many time series draconitic errors cannot be distinguished by seasonal signals and contribute to them, as already noted by (Rebischung et al., 2012), and beating between draconitic and seasonal harmonics can explain the annual and inter-annual amplitude variations. Draconitic and solar year are in phase every 26 years³ during which the amplitude of the combined signal ranges between 0 and 6.8 mm with a beating effect. The superimposition of the 7 draconitics and 4 solar detected harmonics results in a signal amplitude that ranges from 3 to 27 mm. The wavelength RMS are larger for the detected seasonal harmonics and smaller for the draconitic and tidal harmonics, because seasonal effects present a greater variability. The mean amplitudes are coherent with the values reported by (Ostini, 2012), obtained by the FODITS method proposed in (Ostini et al., 2008).

Two peaks has been found with period of 14 and 28 days that are doubtless related to tidal model errors. The peak at 14 days has been attributed to sub-daily EOP tidal errors by (Ray et al., 2013). The relative motions of the Earth, Moon and Sun cause the tides to vary in numerous tidal cycles, the two most important ones being the spring-neap cycle and the equinoctial cycle. The spring-neap cycle is a 14.77

² Draconitic year is the interval of 1.040 ± 0.008 cycles per year (351.2 ± 2.8 days) needed for the Sun to return to the same point in space relative to the GPS orbital nodes (as viewed from the Earth).

³ $365.25 / (365.25 - 351.2) \approx 26$

day cycle resulting from the tidal influence of the sun and moon either reinforcing or partially cancelling each other (neap tides). The semi-annual equinoctial cycle is caused by the tilt of the Earth, and its orbit around the Sun which leads to higher than average spring tides around the time of the equinoxes (March and September) and lower than average spring tides in June and December. Because of its seasonality this effect cannot be distinguished by other seasonal effects. The Moon crosses the ecliptic at the same node every ~ 27.3 days, and a peak can also be observed at a frequency of 28 days. Finally three peaks are at 41 ($=3 \cdot 14$), 82 ($=6 \cdot 14$) and 163 ($=12 \cdot 14$) days, that can also be related to tidal model errors. A synthesis of the detected signals is reported in Tab. 1.

cpy	harmonics [days]						mean amplitudes [mm]		
	expected			estimated			drac.	solar	tidal
	drac.	solar	tidal	drac.	solar	tidal			
1	351.2	365.3	164.0	355±3	364±10	163±2	3.2	3.1	1.3
2	175.6	182.6	82.0	175±3	180±6	82±1	2.0	1.7	0.8
3	117.1	121.8		118±2	121±5		1.3	1.1	
4	87.8	91.3	41.0	88±2	91±3	41±1	1.1	1.5	0.7
5	70.2	73.1		70±2			1.0		
6	58.5	60.9	27.3	58±1		28±1	1.0		1.1
7	50.2	52.2		50±1	53±1		1.0	0.7	
12			13.7			14±1			1.1

Tab. 1 – Detected signals that are consistent with the solar, draconitic and tidal harmonics.

The remaining signatures could be attributed to other un-modeled effects that must be investigated, such as non tidal loading displacement, high order ionosphere terms and mismodeling effect in GPS attitude models. For example, on remarkable peak is at 66 days, that cannot be related to seasonal, draconitic or tidal effects.

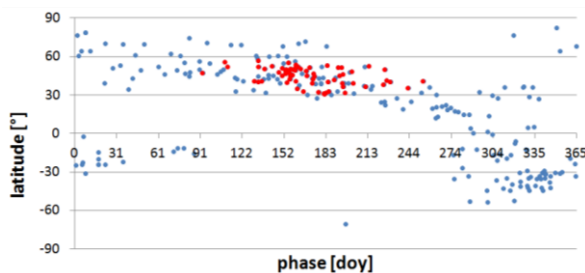


Fig. 6 – Phase of the annual term, in term of doy of the UP maximum. It can be noted some correlation with the station latitude.

The phase ϕ represents the signal maximum in the model [8]. It seems to be spatially correlated, as can be noted in Fig. 6, where the signal phase is represented with respect to station latitudes. The European

cluster is represented in red and has its maximum between day 120 and 220 (April - June). As consequence of the seasonal loading effects, the phase distribution seems to be coherent with the Earth deformation global model proposed by (Blewitt et al., 2001), according to which during February to March the Northern Hemisphere compresses and the Southern Hemisphere expands. The opposite pattern of deformation occurs during August to September. More uniform data from both the hemispheres are necessary to clearly identify this latitude dependant effect.

5 Conclusions

Spectral analysis of weekly station coordinate time series of 526 IGS sites reveals signals at the seasonal, draconitic and tidal harmonics. The analysis has been conducted on the UP component of the REPRO1 time series, while E and N are not yet analyzed and they must be considered in future works. It has been shown that the detected annual signal is spatially correlated in both amplitude and phase, and it depends on the loading changes due to the water cycle. Similar analysis must be conducted on the sub annual signals, in order to better understand their origin, that seems to be related to model errors. Some geophysical effect can also be observed at a global level, such as the expansion of the hemispheres during the summer and their contraction during winter. Other non periodical geophysical signals can be potentially discovered in the long term signal models, not studied in the present work.

6 References

- Albertella, A., B. Betti, F. Sansò, V. Tornatore (2006). Real time and batch navigation solutions: alternative approaches. *Bollettino SIFET*, n. 2 - 2006.
- Blewitt G., D. Lavallée, P. Clarke, K. Nurutdinov (2001). A New Global Mode of Earth Deformation: Seasonal Cycle Detected. *Science* 14 December 2001: Vol. 294 no. 5550. doi: 10.1126/science.1065328
- Collilieux, X., Altamimi, Z., Coulot, D., Ray, J., and Sillard, P. (2007). Comparison of VLBI, GPS, SLR height residuals from ITRF2005 using spec-

- tral and correlation methods. *Journal of Geophysical Research*, Vol. 112, B12403, doi: 10.1029/2007JB004933
- Collilieux, X., L. Métivier, Z. Altamimi, T. van Dam and J. Ray (2010) Quality assessment of GPS reprocessed Terrestrial Reference Frame, *GPS Solutions*, doi:10.1007/s10291-010-0184-6
- Fritsche M., R. Dietrich, A. Rülke, M. Rothacher, P. Steigenberger (2009). Low-degree earth deformation from reprocessed GPS observations. *GPS Solutions*. doi:10.1007/s10291-009-0130-7
- Gazeaux, J., S. Williams, M. King, M. Bos, R. Dach, M. Deo, A.W. Moore, L. Ostini, E. Petrie, M. Roggero and F.N. Teferle (2013). Detecting offsets in GPS time series: first results from the Detection of Offsets in GPS Experiment, *Journal of Geophysical Research - Solid Earth*, doi: 10.1002/jgrb.50152, Online ISSN: 2169-9356.
- Mtamakaya, J.D. (2012). Assessment of atmospheric pressure loading on the international GNSS REPRO1 solutions periodic signatures, Tech Report 282, Department of Survey Engineering, University of New Brunswick, Fredericton.
- Mignard, F. (2003). FAMOUS, Frequency Analysis Mapping On Unusual Sampling, (OCA Cassiopee), Technical report, Obs. de la Cote d'Azur Cassiopee, Nice, France⁴.
- Ostini, L., R. Dach, M. Meindl, S. Schaer, U. Hugentobler (2008). FODITS: A New Tool of the Bernese GPS Software to Analyze Time Series. EUREF 2008 Symposium, Brussels.
- Ostini, L. (2012). Analysis and Quality Assessment of GNSS-Derived Parameter Time Series. Ph.D. dissertation, Philosophisch naturwissenschaftlichen Fakultät der Universität Bern.
- Pagiatakis, S.D. (1999). Stochastic significance of peaks in the least-squares spectrum. *Journal of Geodesy*, 73, 67-78.
- Pagiatakis, S.D. (2000). Application of the least-squares spectral analysis to superconducting gravimeter data treatment and analysis; Proceedings of the workshop on High precision gravity measurements with application to geodynamics and Second GGP workshop, *Cahiers Du Centre Europeen De Geodynamique et de Seismologie (ECGS)*, 17, 103-113.
- Perfetti, N. (2006). Detection of station coordinates discontinuities within the Italian GPS Fiducial Network. *Journal of Geodesy*, Springer Berlin / Heidelberg ISSN 0949-7714 (Print) 1432-1394 (Online).
- Ray, J.R., Z. Altamimi, X. Collilieux, T. van Dam (2008). Anomalous harmonics in the spectra of GPS position estimates. *GPS Solutions*. doi:10.1007/s10291-007-0067-7
- Ray, J., J. Griffiths, X. Collilieux and P. Rebischung (2013) Subseasonal GNSS Positioning Errors, *Geophysical Research Letters*, 40(22), p. 5854-5860, doi:10.1002/2013GL058160
- Rebischung, P., X. Collilieux, T. van Dam, J. Ray, Z. Altamimi (2012). Analysis effects in IGS station motion time series. Presented at *IGS workshop 2012*, Olsztyn, Poland.
- Roggero, M. (2008). Kinematic GPS batch processing, a source for large sparse problems, In: *VII Hotine Marussi Symposium on Theoretical and Computational Geodesy*, Springer-Verlag Berlin and Heidelberg GmbH & Co. K (DEU), 2008, ISBN: 3-540-74583-1.
- Roggero, M. (2012). Discontinuity detection and removal from data time series. In: *VII Hotine Marussi Symposium on Theoretical and Computational Geodesy*, Springer-Verlag Berlin and Heidelberg GmbH & Co. K (DEU), ISBN: 9783642220777.
- Steigenberger, P. (2009), Reprocessing of a global GPS network, Ph.D. dissertation, Fakultät für Bauingenieur und Vermessungswesen, TU München.
- Teunissen, P. (1998). Quality control and GPS. *GPS for Geodesy*, Teunissen P.J.G., Kleusberg A. eds., Springer-Verlag, Berlin, Heidelberg, New York, ISBN 3-540-63661-7.
- Tregoning, P., and C. Watson (2009), Atmospheric effects and spurious signals in GPS analyses, *J. Geophys. Res.*, 114, B09403, doi:10.1029/2009JB006344.
- Vaniček, P., (1969). Approximate spectral analysis by least-squares fit. *Astrophysical Space Science* 4:387-391
- Vaniček, P., (1971). Further development and properties of the spectral analysis by least squares. *Astrophysical Space Science* 12:10-33
- Wells, D., P. Vaniček and S. Pagiatakis (1985). Least squares spectral analysis revisited. Tech Report 84, Department of Survey Engineering, University of New Brunswick, Fredericton.

⁴<http://ftp.obs-nice.fr/pub/mignard/Famous/>
http://obswww.unige.ch/~eyer/VSWG/Meeting4/MINUTES/VSWG4_FM2.pdf